JOURNAL OF APPLIED ELECTROCHEMISTRY 17 (1987) 385–397

Electrochemical study of mass transfer in Li–Mg and Li–Mg–Al alloys

Y. IWADATE*, M. LASSOUANI, F. LANTELME, M. CHEMLA

Laboratoire d'Electrochimie, U.A.430, Université Pierre et Marie Curie, 4 Place Jussieu, 75230 Paris Cedex 05, France

Received 25 July 1985; revised 26 March 1986

The interdiffusion coefficients in Li–Mg alloys and Li–Mg–Al alloys were evaluated using transient techniques such as chronopotentiometry and chronoamperometry. Anodic or cathodic pulses were imposed on the alloy electrodes under galvanostatic and potentiostatic conditions.

Taking into account charging of the double layer, ohmic drop, adsorption of diffusing species and electrolyte–electrode boundary shift, the diffusion coefficients of lithium in Li–Mg alloys (α-phase and β-phase) and in Li–Mg–Al alloys were estimated at around 420° C. In the case of Li–Mg α-phase alloys, the values of the diffusion coefficients, D_{Li}, can be represented in a polynomial expansion of the composition of the alloy, X_{Li} (mol %) as follows:

$$\ln D_{Li} = -19.850 - 0.4294 X_{Li} + 0.0249 X_{Li}^2$$

The diffusion coefficients of lithium in Li–Mg (β-phase) alloys show extremely large values ($\simeq 10^{-6}$ cm^2 s^{-1}) as also in the Li–Al β-phase alloys.

1. Introduction

The most electroactive element, lithium, is presently being considered for use as an anode material for high temperature batteries in which molten salts are utilized as electrolytes; molten salt batteries are being developed for load levelling and for use as power sources for electric vehicles [1–4]. However, some difficulties exist in developing and designing these batteries since the melting points of such electrolytes are in general higher than that of lithium, and the lithium metal itself is highly corrosive towards the cell materials. In addition, appreciable dissolution of lithium into molten chloride electrolytes causes self-discharge. These difficulties can be avoided by using solid lithium alloys as anode materials. Up to the present, lithium alloys such as Li–Al, Li–Si, Li–B and Li–Ge have been generally recognized to be candidate materials [5–11]. The utility of these alloys consists of the facts that they are in solid aggregate state, less corrosive even at elevated temperature and show an insignificant decrease in voltage (about 300 mV) relative to pure lithium.

Special attention must be paid to the Li–Mg alloys phase diagram shown in Fig. 1 since it reflects on their mechanical properties. These alloys are ductile compared with the other lithium alloys. The ductility facilitates production of anodes and achievement of molten salt batteries. Similar situations may be expected for Li–Mg–Al alloys, and also the introduction of magnesium into the Li–Al alloy decreases its brittleness and makes the preparation of anodes for chemical current sources easier.

As the situation now stands, there are few data on the thermodynamic and electrochemical behaviour of binary Li–Mg and ternary Li–Mg–Al alloys [12–15]. Sahoo and Atkinson [16] have recently studied the preparation and fabrication of Li–Mg alloys and concluded that additions of

* *Present address*: Chiba University, Department of Synthetic Chemistry, Faculty of Engineering, 1-33 Yayoi-Cho, Chiba, Japan 260.

0021-891X/87 $03.00 + .12

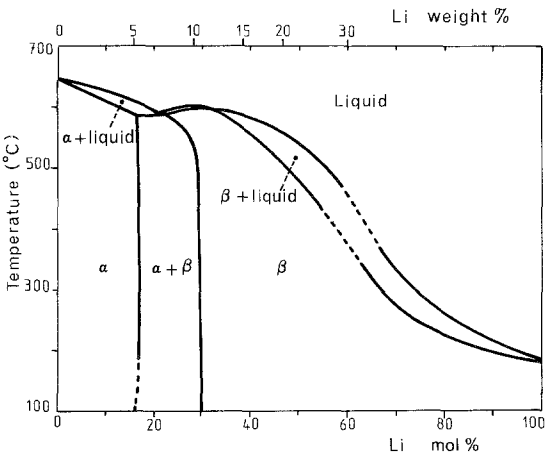

Fig. 1. The Mg–Li equilibrium phase diagram.

just over 10 wt % (28 mol %) lithium to magnesium cause its crystal structure to become cubic and render the alloy readily workable. It has also been reported that single-phase alloys (β-phase), including those with lower lithium content, have a corrosion resistance similar to the other magnesium-based alloys and give higher voltages and better discharge characteristics in the range 6.5 to 12 wt % (19.6 to 32.3 mol %) of lithium. For these reasons, it is important to investigate the diffusion behaviour as well as the thermodynamic properties of the Li–Mg and Li–Mg–Al alloys in order to clarify the mechanism of transport in the solid state and to advance the realization of molten salt batteries.

2. Experimental details

2.1. *Electrode preparation*

The Li–Mg electrodes were made from a magnesium rod which was alloyed with lithium to a definite concentration by high temperature electrolysis at a constant potential. For Li–Mg–Al anodes, samples of Mg–Al alloys were used as the starting materials for the working electrodes. They were prepared beforehand by the following procedure: accurately weighed magnesium and aluminium specimens were degreased with acetone and introduced into a vitreous carbon vessel. The specimens were kept under vacuum for 1 h at room temperature and then heated to 550° C under reduced pressure for 2 h; argon gas was introduced into the cell which was then heated to 800° C. After melting the specimens, the homogeneous liquid alloy was degassed under vacuum for a few minutes so as to prevent the presence of any bubbles in the final sample. Then argon gas was introduced to the cell as soon as possible owing to the appreciable vaporization of the metals, and the melt was rapidly cooled to 550° C and then maintained at that temperature for 2 h. Finally, the furnace was switched off to anneal the alloy for more than 12 h. The accurate composition was ascertained to be unchanged by means of an atomic absorption spectrometer.

2.2. *Electrochemical apparatus*

The schematic diagram of the electrochemical cell has already been described in a previous publication [17]. The components of the apparatus were selected in order to achieve a sufficiently vacuum-tight cell even at elevated temperature; in fact the residual pressure was less than 0.1 mm Hg at 500° C. The electrolyte was a LiCl (59 mol %)–KCl (41 mol %) eutectic melt. The constituent salts were accurately weighed, carefully dehydrated under reduced pressure and finally purified by

premelting under an HCl atmosphere. During each experimental run, argon gas was kept flowing throughout the cell.

The detailed procedure of preparation and purification has already been described by Laitinen *et al.* [18] as well as in our previous work [19].

In the present work a chlorine gas electrode (Cl_2/Cl^-) was employed as reference. Its potential versus the Li/Li^+ electrode was found to be +3.650 V. The counter electrode was made from a graphite rod separated from the main compartment by a quartz frit in order to avoid a direct reaction between chlorine gas and the metallic electrodes.

The electrical pulses were supplied by a galvanostat–potentiostat (Amel Model 555) with a rapid response (10 μs) which was connected to a function generator (Amel Model 565). The signals of potential or current versus time were recorded by means of a storage oscilloscope (Tektronix 7023) or a digital memory recorder (Biomation 805).

3. Theoretical background and analytical method

When the lithium alloy electrode, immersed in the electrolyte, is in the equilibrium state, the potential, E_{eq}, is given by the Nernst equation:

$$E_{eq} = E^\circ + (RT/F) \ln (a^*_{ox}/a^*_{red}) \tag{1}$$

where a^*_{ox} and a^*_{red} are the activities of the oxidized species (Li^+) in the electrolyte and the reduced species (Li) existing in the alloy electrode, respectively. If not at equilibrium the potential, E, takes the following form, the electron transfer being rapid at this temperature.

$$E = E_{eq} + (RT/F) \ln (a_{ox} a^*_{red}/a^*_{ox} a_{red}) \tag{2}$$

3.1. *Chronopotentiometry*

When a galvanostatic pulse of current density, i, is imposed for time, t, the potential variation of the alloy electrode versus time is given by [19, 20]:

$$\eta = E - E_{eq} = \frac{RT}{F} \ln \frac{[C^*_{ox} + 2i(t^{\frac{1}{2}}/F)(\pi D_{ox})^{\frac{1}{2}}] f^*_{red} C^*_{red}}{[C^*_{red} - 2i(t^{\frac{1}{2}}/F)(\pi D_{red})^{\frac{1}{2}}] f_{red} C^*_{red}} \tag{3}$$

Where the superscript $*$ refers to the equilibrium situation, and f_{red} is the activity coefficient satisfying the relation $a_{red} = f_{red} C_{red}$. The values of f_{red} versus C_{red} have been evaluated previously from the results of Tiunov [13]. As the variations of C_{ox} are always very small, it is not necessary to take account of the f_{ox} factors. The quantities C^*_{ox}, C^*_{red}, D_{ox} were known from previous work [19]. Thus Equation 3 was used to calculate D_{red}.

At the end of the pulse, when the current is switched off, the potential recovery back to the equilibrium situation can be used to determine the interdiffusion coefficient, D_{red}. The concentration variation has been reported by Berzins and Delahay [22]; at the electrode surface the time dependence of the concentration is

$$C_{red} = C^*_{red} + \frac{2i}{nF(\pi D_{red})^{\frac{1}{2}}} [(\theta + t)^{\frac{1}{2}} - (t)^{\frac{1}{2}}] \tag{4}$$

where θ is the pulse duration.

The value of D_{red} is calculated from Equation 4 by a trial and error method, the variation of C_{red} being known from the potential response.

3.2. *Chronoamperometry*

When an abrupt change, η, of potential is imposed, the current density flowing through the electrolytic cell is given by the Cottrell relation:

$$\begin{aligned} i &= F(C^*_{red} - C_{red})(D_{red}/\pi t)^{\frac{1}{2}} \\ i &= F(C_{ox} - C^*_{ox})(D_{ox}/\pi t)^{\frac{1}{2}} \end{aligned} \tag{5}$$

As D_{ox} is known, it is possible to calculate C_{ox}. Moreover, the ratio $f_{ox}C_{ox}/f_{red}C_{red}$ at the electrode surface is automatically fixed by the constant potential impulse. Then the value of D_{red} is deduced from the Cottrell relation [23].

In electrochemical techniques, diffusion phenomena can only take place when deposition or dissolution of electroactive species occurs; that is, the velocity and the direction of the electrolyte–electrode interface movement are dependent upon the magnitude of the current which may be either anodic or cathodic. A correction was therefore required to account for electrode boundary movement [21], according to the method recommended by Oldham and Raleigh [24] for the potentiostatic experiments and by Godulyan and Zatsepin [25] for the galvanostatic experiments.

4. Results

The determination of the alloy composition and the estimation of the diffusion coefficient from electrical potential measurements require a reliable evaluation of the activity coefficients of the diffusing species.

4.1. *Thermodynamics of alloys*

In this section, the data are taken from the literature [13] with a few modifications so as to adjust the thermodynamical results which are expressed by the polynomial expansion [27]:

$$\ln \gamma_{Li} = \alpha_0 + \alpha_1(1 - X) + \alpha_2(1 - X)^2 + \alpha_3(1 - X)^3 + \ldots \tag{6}$$

The experimental results could be represented with sufficient accuracy by neglecting the terms higher than third order. The coefficients α_0, α_1, α_2 and α_3 for the Li–Mg alloys (α-phase and β-phase), which are evaluated by a least-squares method, are listed in Table 1.

The activity, a_{Li}, in the alloy is related to the atomic fraction, X_{Li}, by

$$a_{Li} = \gamma_{Li}X_{Li} \tag{7}$$

where γ_{Li} is the activity coefficient. X_{Li} permits the derivation of the molar concentration

$$C_{Li} = X_{Li}\varrho_{Li-Mg}/[X_{Li}M_{Li} + (1 - X_{Li})M_{Mg}] \tag{8}$$

where ϱ_{Li-Mg} is the alloy specific mass, and M_{Li} and M_{Mg} are the atomic masses of lithium and magnesium, respectively.

Table 1. Coefficients of the polynomial expansion (Equation 6) expressing the dependence of the activity coefficients, γ_{Li}, on the lithium mole fraction, X, of the Li–Mg alloys

	α_0	α_1	α_2	α_3
α-phase ($0 < X < 0.18$)	−17.311	85.905	−124.12	52.129
β-phase ($0.30 < X < 0.45$)	−1.939	10.85	−22.79	12.53

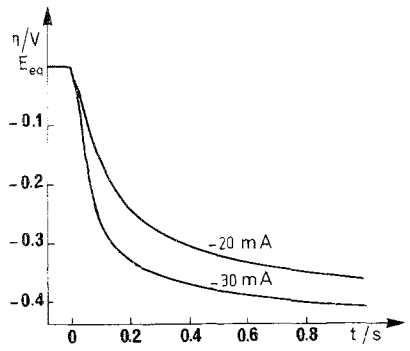

Fig. 2. Chronopotentiogram of α-phase Mg–Li alloy. E_{eq} = 0.618 V/Li; X_{Li}^{*} = 0.1 mol %; T = 420° C, S = 1.4 cm^2.

4.1.1. Galvanostatic method. A concentration gradient was created at the electrode surface by imposing a cathodic current pulse with a well-defined amplitude, I, and duration, θ [26]. The potential variation resulting from the concentration gradient is related to the diffusion of lithium from the surface to the inside of the matrix, as indicated by Equation 3. The values of I and θ must be small enough to produce only a slight variation of the concentration, since a large perturbation of the electrode surface must be avoided. This technique has already been used for different compositions of the α- or β-phases in Al–Li alloys (see previous paper [19]).

The experimental results were represented by curves which could be stored either as photographs of an oscilloscope screen or as numerical data in a digital recorder memory. Each curve represented the potential variation as a function of time during the current pulse, and supplied information on the transport properties of the electroactive species. In fact, depending on the experimental conditions, it was possible to obtain both the diffusion coefficient of Li^+ in the electrolyte and the interdiffusion coefficient of lithium atoms in the alloy.

When the deposition method is used, there is an increase of the concentration of lithium at the surface of the electrode. The potential then changes slowly when the concentration reaches the lithium-rich region (Fig. 2). In contrast, when an anodic current flows, the relative change of concentration C_{Li}/C_{Li}^{*} becomes very large, particularly at the end of the pulse when C_{Li} approaches zero. This results in an abrupt variation of the potential which is shown in Fig. 3. Since the phenomenon is controlled by diffusion, the application of Equation 3 permits the determination of the diffusion coefficient from the chronopotentiogram. In the case shown in Fig. 3, one must distinguish the ascending part corresponding to the current flow up to the time θ from the descending part describing the return to the equilibrium potential when current has been switched off. The latter part of the curve, which corresponds to diffusion without current, can be analysed by Equation 4.

4.1.2. Potentiostatic method. The curves reported in Fig. 4 represent the variation of I when an abrupt change of potential is imposed on an Li–Mg alloy electrode. The surface concentration, C_{Li},

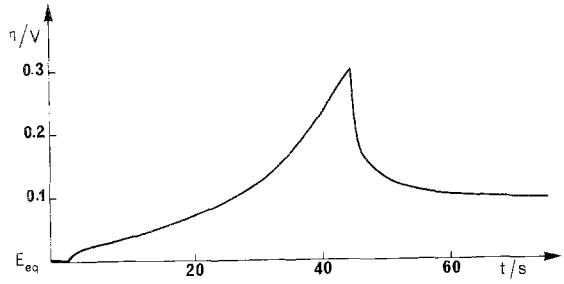

Fig. 3. Chronopotentiogram of α-phase Mg–Li alloys. E_{eq} = 0.205 V/Li; X_{Li}^{*} = 17.3 mol %; T = 420° C; S = 1.15 cm^2. First part: t < 44 s; I = +2 mA. Second part: t > 44 s; I = 0.

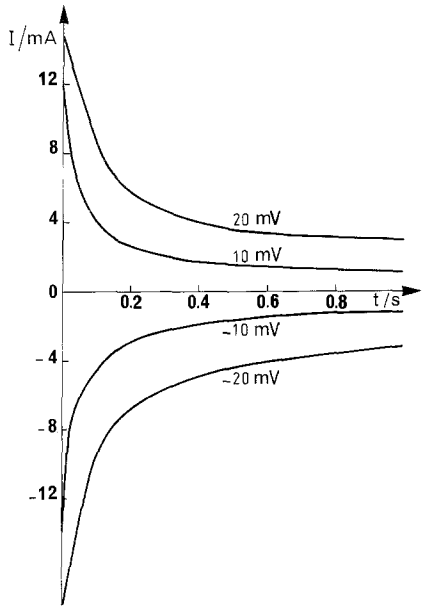

Fig. 4. Chronoamperograms of α-phase Mg–Li alloys. E_{eq} = 0.205 V/Li; X_{Li}^{*} = 17.3 mol %; T = 420° C; S = 1.15 cm^2.

depends on the amplitude of the potential step, which is generally a few millivolts so as to result in a slight variation of the concentration and thus to avoid the difficulties arising from the concentration dependence of D. The graphical representation of I against $t^{-\frac{1}{2}}$ obeys the Cottrell relation. In practice, the slope of the straight line derived from the Cottrell relation is equal to $F(C_{red}^{*} - C_{red})(D_{red}/\pi)^{\frac{1}{2}}$. The values of D do not change appreciably with the amplitude or the sign (oxidation or reduction) of the imposed potential jump.

4.1.3. Comparison with previous results. Protasov *et al.* [12] have obtained diffusion coefficients in Li–Mg alloys (β-phase) under galvanostatic conditions using LiCl–KCl, LiCl–KCl–CsCl and LiF–LiCl–LiBr eutectic melts as electrolytes. Their values, estimated at 420° C by interpolation, are about 1.6 × 10^{-6} (58 Li mol %), 5.6 × 10^{-7} (43 Li mol %) and 1.3 × 10^{-7} (31 Li mol %) cm^2 s^{-1}.

The diffusion coefficients of lithium in the α-phase obtained from our work range from nearly 10^{-9} to 10^{-10} cm^2 s^{-1}, and those in the β-phase are of the order of 10^{-6} cm^2 s^{-1}.

5. Discussion

The application of the classical laws of chronoamperometry or chronopotentiometry is affected by certain factors such as charging of the double layer, adsorption, the presence of impurities and the contribution of other electroactive species such as Mg^{2+}. The last two factors have no influence on the electrochemical results beyond the experimental errors of the method. The first two factors introduce some perturbation only for the short-time responses. The main effect arises from the presence of electroactive adsorbed species. but it turns out to be negligible for times longer than 20 ms.

5.1. *Concentration dependence of the diffusion coefficient*

The method provided evidence for the variation of the diffusion coefficient with alloy composition (α- or β-phase) by using alloy electrodes of varying lithium content as tabulated in Tables 2, 3 and 4.

Table 2. Diffusion constants from galvanostatic experiments in Li–Mg alloys at 420° C. D_{corr} takes account of the boundary shift correction

Conditions	I *(mA)*	D_{Sand} $(\times 10^{-10}\,cm^2\,s^{-1})$	D_{corr} $(\times 10^{-10}\,cm^2\,s^{-1})$
E_{eq} = 0.205 V/Li	2	4.4	3.8
	5	8.7	7.7
X_{Li}^* = 17.3 mol %	25	7.4	6.4
S = 1.14 cm^2	140	6.9	6.0
E_{eq} = 0.250 V/Li	−30	9.8	8.4
	−70	21.5	18.4
X_{Li}^* = 13.2 mol %	30	3.6	3.1
S = 1.38 cm^2	50	3.3	2.8
E_{eq} = 0.580 V/Li	−15	13	12
	−30	9.7	9.2
X_{Li}^* = 0.17 mol %	−70	8.7	7.7
S = 1.38 cm^2	−100	9.9	8.5

Within each phase a continuous variation of D_{Li} is observed against X_{Li} mol %. For the α-phase, the smoothed expression for the experimental values of D_{Li} is:

$$\ln D_{red} = -19.850 - 0.4294X_{Li} + 0.0249X_{Li}^2 \quad (9)$$

where the standard deviation on ln D is ± 0.7.

Table 3. Diffusion constants from potentiostatic transients on Li–Mg alloys α-phase at 420° C. D_{corr} account for the correction of the boundary shift

Conditions	η *(mV)*	X_{Li} *(mol %)*	$D_{Cottrell}$ $(\times 10^{-10}\,cm^2\,s^{-1})$	D_{corr} $(\times 10^{-10}\,cm^2\,s^{-1})$
E_{eq} = 0.205 V/Li	10	16.5	11	7.5
	20	15.6	14	9.5
X_{Li}^* = 17.3 mol %	50	12.9	9.9	7.0
E_{eq} = 0.250 V/Li	−50	17.8	49	36
	−20	15	16	12
X_{Li}^* = 13.2 mol %	−10	14.1	7.7	6.0
	10	12.4	5.8	4.4
	20	11.6	8.9	6.8
	50	9.1	11.5	8.8
E_{eq} = 0.300 V/Li	−50	13.3	4.8	3.9
	−20	10.7	2.3	1.9
X_{Li}^* = 9.13 mol %	20	7.6	3.1	2.6
	50	5.6	2.8	2.3
E_{eq} = 0.350 V/Li	−50	9.1	1.9	1.7
	−20	6.9	3.0	2.7
X_{Li}^* = 5.61 mol %	−10	6.3	1.5	1.3
	10	5.0	2.4	2.2
	20	4.5	3.8	3.4
	50	3.0	5.6	5.0

Table 4. Diffusion constants from potentiostatic transients on Li–Mg alloys (β-phase) at 420° C. $X_{Li}^{*} = 34.1$ *mol %;* $E_{eq} = 0.130$ *V/Li*

η (mV)	X_{Li} (mol %)	$D_{Cottrell}$ (10^{-6} cm^2 s^{-1})	D_{corr} (10^{-6} cm^2 s^{-1})
20	28.5	5.0	2.2
10	31.3	1.8	0.8
−10	37.1	3.0	1.3
−15	38.5	5.0	2.2

In Tables 2, 3 and 4 the D_{red} values are modified on the basis of the boundary shift correction as explained previously [21]. The boundary shift has little influence on the results measured under galvanostatic conditions. In most cases, the deviation of the corrected value from that derived by the Sand equation is found to be less than 15%, as shown in Table 2.

In contrast, the effect is important in the calculation of the diffusion coefficient of lithium under potentiostatic conditions. As indicated in Table 3, the diffusion coefficient derived from the Cottrell equation is nearly 30% larger than the corresponding value obtained on the basis of the calculating method of Oldham and Raleigh [24].

A large scatter is observed in the experimental data of the lithium diffusion coefficients. This is probably due to the variable influence of the grain boundary contribution to the lithium transport into the alloy.

On the other hand, it is found that the diffusion coefficients in the β-phase are extremely large in comparison with those in the α-phase in spite of the solid state diffusion proceeding in both cases. In fact, it is found that the diffusion rates in the β-phase are nearly equivalent to those observed in the liquid state. This drastic increase (the boundary between α + β-phase and β-phase is positioned at 29.9 mol % lithium at 420° C) is ascribed to the contribution of the structure breaking arising from the phase transition process.

5.2. *Analysis of results obtained by the galvanostatic method*

The potential variation during an anodic impulse of current, which results in the depletion of lithium from the electrode surface, is considered. After the transition time, τ, the surface concentration of the electroactive species, given by Equation 3, reaches a value near zero, which induces a steep variation of the potential (Fig. 3). Neglecting the variations of concentration in the liquid phase, the following treatment is available to fit the potential variation versus time, t:

$$\begin{aligned} \eta &= (RT/nF) \ln (a^{*}_{red}/a_{red}) \\ \eta &= -(RT/nF) \ln \frac{f}{f^{*}} \left[\frac{(\tau)^{\frac{1}{2}} - (t)^{\frac{1}{2}}}{(\tau)^{\frac{1}{2}}} \right] \end{aligned} \tag{10}$$

The transition time, τ, which is determined according to the usual graphical method [28], allows a plot of η versus $\ln f/f^{*}\{[(\tau)^{\frac{1}{2}} - (t)^{\frac{1}{2}}]/(\tau)^{\frac{1}{2}}\}$ (Fig. 5). Although this graph is not a perfect straight line, the value of the estimated slope leads to a value of $n = 1.1$ which agrees with a fast, one-electron transfer. It can also be seen from Fig. 5 that, if the influence of activity coefficients is neglected, the error on the estimated value of n may reach 40%.

For high current densities deviations from the Sand law are observed, showing a noticeable increase of the product $i\tau^{\frac{1}{2}}$. This effect does not arise from double-layer charging. Indeed, in fused salts the conductivity is high and the concentration of electroactive species is very large; thus the duration of the charging of the double layer is neglibible at the time scale of the experiments. This

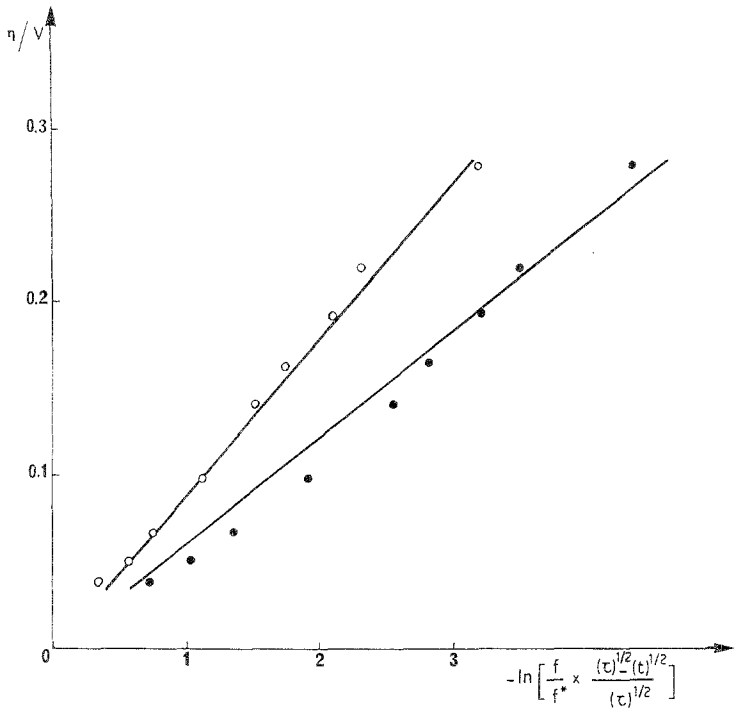

Fig. 5. Analysis of the chronopotentiogram after a galvanostatic pulse on a Mg–Li alloy. Open circles, f equal to f^*; full circles, values of f and f^* extracted from [13].

deviation from the classical laws at short time observations is attributed to the existence of an adsorbed layer of electroactive species. When adsorption takes place on the electrode, the faradic current is the sum of two contributions according to the origin of the reacting ions:

$$i = i_{ads} + i_{dif} \tag{11}$$

where i_{ads} and i_{dif} refer to the current densities for the adsorption and diffusion steps. Under galvanostatic conditions the faradic current is first used for the discharge of ions in the adsorbed layer. The total transition time is then expressed as

$$i\tau = (F^2\pi D/4)(C^2/i) + F\Gamma_{eq} \tag{12}$$

The intercept and the slope of the straight line obtained by drawing $i\tau$ against C^2/i leads to the surface concentration of the adsorbed species, Γ_{eq}, and the diffusion coefficient, D, of the electroactive solute species. This model has been proposed by Laitinen [29] and was for the interpretation of our results as shown on Fig. 6, from which we could derive:

$$\Gamma_{eq} = 4.46 \times 10^{-8}\,\text{mol cm}^{-2}$$

and

$$D = 2.46 \times 10^{-10}\,\text{cm}^2\,\text{s}^{-1}$$

This result demonstrates neatly the existence of an adsorbed layer of lithium atoms at the interface of a Li–Mg α-phase alloy with the molten LiCl–KCl electrolyte.

5.3. *Analysis of results obtained by the potentiostatic method*

As seen in Fig. 7, the Cottrell law is generally well fitted for observation times beyond about 20 ms. When an overpotential is imposed to an electrochemical reaction controlled by diffusion, the current

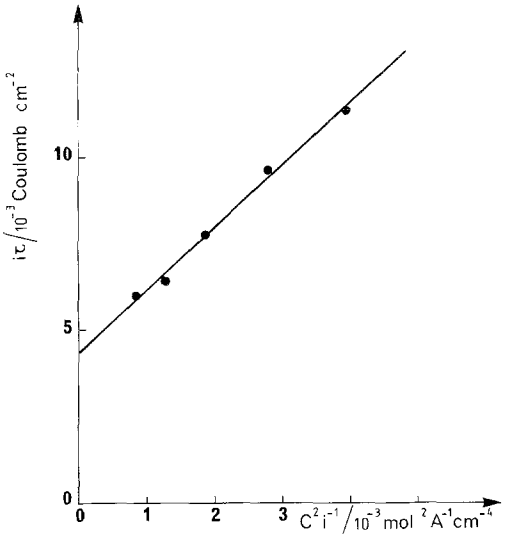

Fig. 6. Determination of the amount of adsorbed lithium.

density and the overpotential are expressed as

$$\begin{aligned} i &= F(C^*_{red} - C_{red})\,(D_{red}/\pi t)^{\frac{1}{2}} \\ \eta &= -(RT/F)\ln\,(a_{red}/a^*_{red}) \end{aligned} \tag{13}$$

Then,

$$C^*_{red} - C_{red} = C^*_{red}\{1 - \exp\,[-F(\eta + K)/RT]\} \tag{14}$$

where

$$K = (RT/F)\ln\,(f/f^*) \tag{15}$$

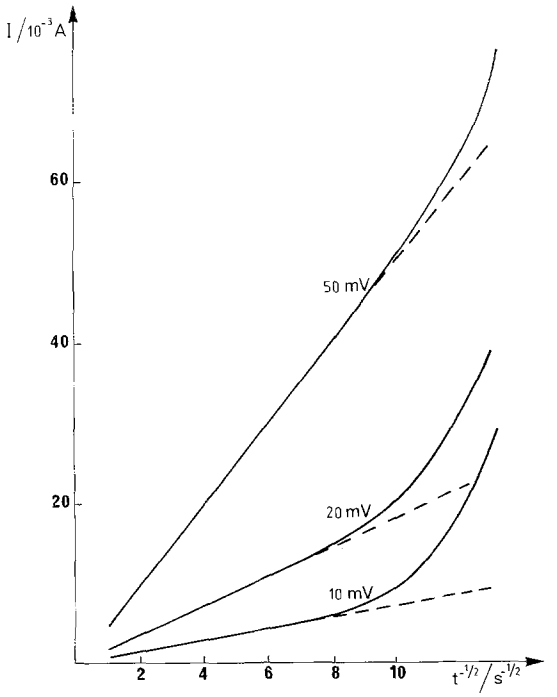

Fig. 7. Evidence for adsorption phenomenon by analysis of the response after a potentiostatic pulse.

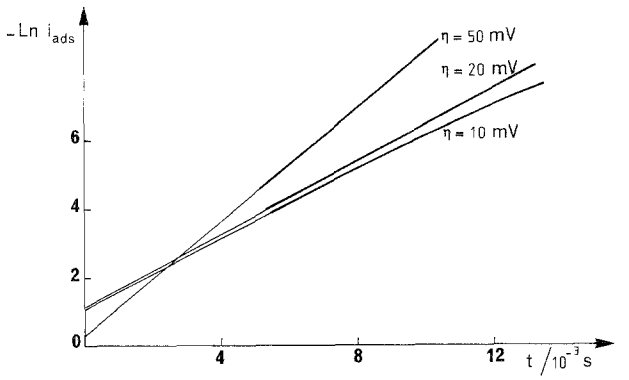

Fig. 8. Kinetics of oxidation of lithium in the adsorption layer.

The final expression is obtained by substitution of Equation 14 into Equation 13:

$$i = FC^*_{red}\{1 - \exp[-F(\eta + K)/RT]\}(D_{red}/\pi t)^{\frac{1}{2}} \quad (16)$$

For small values of η the corrective term, K, is insignificant since f is very close to f^* in magnitude. For high values of overpotential the whole exponential term is very small and, again, the influence of activity coefficients is negligible.

A behaviour similar to that observed with the galvanostatic method is again observed, i.e. a significant deviation for the Cottrell law appears for times shorter than 15 ms, which cannot be assigned to the response of the apparatus ($\simeq 10\,\mu$s) nor to the capacity of the double layer (2×10^{-4} F cm^{-2}). This deviation is assumed to result from the oxidation current of an adsorbed layer of lithium atoms at the surface of the alloy electrode. The adsorption current, i_{ads}, is a measurement of the rate of depletion of the adsorbed layer [30], while the diffusion current, i_{diff}, is determined by the Cottrell law. Thus the total current density, under potentiostatic conditions, is

$$i = -F(d\Gamma/dt) + FD^{\frac{1}{2}}C/(\pi t)^{\frac{1}{2}} \quad (17)$$

Assuming that the electrochemical oxidation of the adsorbed species is a first order reaction, then

$$d\Gamma/dt = -k\Gamma \quad (18)$$

Finally we obtain

$$i = Fk\Gamma_{eq}\, e^{-kt} + FD^{\frac{1}{2}}C/(\pi t)^{\frac{1}{2}} \quad (19)$$

where k is the reaction rate constant, at the imposed potential. Its value is estimated from results given in Fig. 8 which lead to:

$$k = 6.2 \times 10^2\,s^{-1}$$

and

$$\Gamma_{eq} = 7.2 \times 10^{-9}\,mol\,cm^{-2},$$

the value of Γ_{eq} being in fair agreement with that obtained under galvanostatic conditions.

5.4. *Tentative determination of the diffusion coefficients in Li–Mg–Al alloys*

As indicated previously, there are few data on the diffusion coefficients of lithium in Li–Mg–Al alloys. Those reported by Protasov *et al.* [14] correspond to the following compositions of alloy Li–Mg–Al, expressed in mol %: 50 : 10 : 40, 50 : 25 : 25 and 50 : 40 : 10. In the present work, lithium atoms were introduced into a Mg–Al alloy electrode at a given composition by imposing a cathodic

Table 5. Coefficients for the polynomial expansion expressing the dependence of the activity coefficients, γ_{Li}, on the lithium mole fraction, X, in the Li–Mg–Al alloys (Equation 23)

Y_{Al} (mol %)	Y_{Mg} (mol %)	A_0	A_1	A_2	A_3	A_4
32	68	211.31	−861.39	1278.1	−808.10	175.65
10	90	54.13	−210.12	314.08	−216.69	54.89

potential. Using the same method as before, the diffusion coefficients were estimated for both cathodic and anodic processes. However, according to Rowland *et al.* [31], Li–Mg–Al alloys possess many phases which causes difficulty in the evaluation of the alloy composition. Moreover, it is necessary to estimate the values of ln γ expressed as a polynomial expansion versus the alloy composition. In our calculation, we assume that the activity coefficient of lithium in the ternary Li–Mg–Al alloy can be estimated from those in the binary Li–Al [32] and Li–Mg α-phase alloys. However, we must point out that the α-phase of the Li–Al alloy ranges only from 0 to about 10 Li at %. Therefore, the calculation is only available for concentrations not exceeding this limit.

If the activities of lithium atoms in the binary alloys are written as

$$a_1 = \gamma_1 X \quad \text{and} \quad a_2 = \gamma_2 X \tag{20}$$

where γ_1 and γ_2 are the activity coefficients of lithium in each alloy and X is the atomic fraction of lithium, our procedure consists of estimating the mean activity in the ternary alloy as being equal to the geometrical average of these values

$$a_m = \gamma_m X \quad \text{with} \quad \gamma_m = \gamma_1^y \gamma_2^{1-y} \tag{21}$$

where y is the atomic fraction of aluminium in the original Mg–Al alloy, and γ_m is the mean activity coefficient of lithium. The polynomial coefficients for the Li–Al and Li–Mg binary alloys are written as

$$\ln \gamma_1 \quad \sum_0^4 \alpha_{1i}(1 - X)^i \tag{22}$$

$$\ln \gamma_2 = \sum_0^3 \alpha_{2i}(1 - X)^i \tag{23}$$

Accordingly, the polynomial coefficients A_0, A_1, A_2, A_3, A_4 for the logarithmic expression of the activity coefficients in the Li–Al–Mg alloys are expressed as

$$A_i = y\alpha_{1i} + (1 - y)\alpha_{2i}$$

$$\ln \gamma_m = A_0 + A_1(1 - X) + A_2(1 - X)^2 + A_3(1 - X)^3 + A_4(1 - X)^4 \tag{24}$$

The mean specific weight, ϱ_m, and the mean molar mass, M_m, of the original Mg–Al alloys are defined as follows:

$$\varrho_m = y\varrho_{Al} + (1 - y)\varrho_{Mg} \tag{25}$$

$$M_m = yM_{Al} + (1 - y)M_{Mg} \tag{26}$$

The numerical data used in the calculation are listed in Table 5 in which the activity coefficients of lithium in the Li–Al α-phase are taken from the previous paper [19].

The data have been used to interpret the behaviour of these alloys under potentiostatic conditions. Results reported in Table 6 indicate that the interdiffusion coefficients are much larger than those observed in binary alloys. The flow rate of lithium is about a hundred times faster in the Li–Mg–Al ternary alloy. This very large increase in the lithium atoms mobility in the Li–Mg–Al ternary alloy can be correlated with the proximity of the melting point ($\simeq 460°$ C) of the Al–Mg alloys studied,

Table 6. Diffusion constants from potentiostatic transients on Li–Mg–Al alloys at 420° C. D_{corr} corresponds to the correction of boundary shift

	η (mV)	X_{Li} (mol %)	$D_{Cottrell}$ (10^{-8} cm^2 s^{-1})	D_{corr} (10^{-8} cm^2 s^{-1})
E_{eq} = 0.250 V/Li	40	9.9	4.7	3.5
X^*_{Li} = 13.5 mol %	20	11.6	3.9	2.9
X^*_{Mg} = 77.8 mol %	−20	15.7	5.0	3.6
X^*_{Al} = 8.7 mol %	−40	18.0	5.5	4.0
E_{eq} = 0.250 V/Li				
X^*_{Li} = 14.9 mol %	40	9.9	6.9	4.9
X^*_{Mg} = 57.9 mol %	20	11.9	5.4	3.8
X^*_{Al} = 27.2 mol %				

whereas for pure aluminium or magnesium the liquid phases appear only at temperatures near 600° C.

Acknowledgements

This work was supported by the CNRS under contract ATP–PIRSEM, 'Application de l'Electricité à la Chimie'. One of the authors (YI) is deeply indebted to the CNRS for a postdoctoral grant.

References

[1] N. P. Yao, L. A. Heredy and R. C. Saunders, *J. Electrochem. Soc.* **118** (1971) 1039.
[2] A. K. Fisher and D. R. Vissers, *ibid* **130** (1983) 5.
[3] F. J. Martino, E. C. Gay and W. E. Moore, *ibid.* **129** (1982) 2701.
[4] E. C. Gay, D. R. Vissers, F. J. Martino and K. E. Anderson, *ibid.* **123** (1976) 1591.
[5] S. D. James, *Electrochim. Acta* **21** (1976) 157.
[6] A. L. L'vov, A. A. Gnilomedov, A. P. Selemenev and E. N. Protasov, *Sov. Electrochem.* **11** (1975) 1232.
[7] M. M. Nicholson, *J. Electrochem. Soc.* **121** (1974) 734.
[8] R. A. Sharma and R. Seefurth, *ibid.* **123** (1976) 1763.
[9] S. D. James and L. E. De Vries, *ibid.* **123** (1976) 321.
[10] E. N. Protasov, A. A. Gnilomedov, A. L. L'vov, A. A. Suchkov and A. S. Ivanos, *Sov. Electrochem.* **17** (1980) 750.
[11] M. R. St. John, A. J. Furgala and A. F. Sammells, *J. Electrochem. Soc.* **129** (1982) 246.
[12] E. N. Protasov, A. A. Gnilomedov and A. L. L'vov, *Sov. Electrochem.* **14** (1978) 1127.
[13] V. S. Tiunov, A. G. Morachevskii and A. I. Demidov, *J. Appl. Chem. USSR* **52** (1979) 2454.
[14] E. N. Protasov, A. A. Gnilomedov, A. L. L'vov and A. S. Ivanov, *Sov. Electrochem.* **15** (1979) 1061.
[15] M. L. Saboungi and M. Blander, *J. Electrochem. Soc.* **122** (1975) 1631.
[16] M. Sahoo and J. T. N. Atkinson, *J. Mater. Sci.* **17** (1982) 3564.
[17] F. Lantelme, J. P. Hanselin and M. Chemla, *Electrochim. Acta* **22** (1977) 1113.
[18] H. A. Laitinen, W. S. Ferguson and R. H. Osteryoung, *J. Electrochem. Soc.* **104** (1957) 516.
[19] F. Lantelme, Y. Iwadate, Y. Shi and M. Chemla, *J. Electroanal. Chem.* **187** (1985) 229.
[20] D. D. MacDonald, 'Transient Techniques in Electrochemistry', Plenum Press, New York (1977).
[21] F. Lantelme, *J. Electroanal. Chem.* **196** (1985) 227.
[22] T. Berzins and P. Delahay, *J. Amer. Chem. Soc.* **75** (1953) 4205.
[23] F. Lantelme and M. Chemla, *Z. Naturforsch.* **38a** (1983) 106.
[24] K. B. Oldham and D. O. Raleigh, *J. Electrochem. Soc.* **118** (1971) 252.
[25] L. B. Godulyan and V. M. Zatsepin, *Sov. Electrochem.* **16** (1980) 1427.
[26] F. Lantelme and S. Belaidouni, *Electrochim. Acta* **26** (1981) 1225.
[27] C. Wagner, 'Thermodynamics of Alloys', Addison-Wesley Inc., Reading, Mass. (1952) p. 47.
[28] W. H. Reinmuth, *Anal. Chem.* **33** (1961) 485.
[29] H. A. Laitinen, *ibid.* **33** (1961) 1458.
[30] W. Lorenz, *Z. Elektrochem.* **59** (1955) 730.
[31] J. A. Rowland, Jr., C. E. Armantrout and D. F. Walsh, *Trans. AIME (J. Metals)* **203** (1955) 355.
[32] C. J. Wen, B. A. Boukamp, R. A. Huggins and W. Weppner, *J. Electrochem. Soc.* **126** (1979) 2258.